Composites: Part B 67 (2014) 84–94

Contents lists available at ScienceDirect

Composites: Part B

journal homepage: www.elsevier.com/locate/compositesb

Functionalized multiwall carbon nanotubes strengthened GRP hybrid composites: Improved properties with optimum fiber content

Jacob Muthu *, Casian Dendere

DST-NRF Centre of Excellence in Strong Materials and RP/Composites Facility, School of Mechanical, Industrial and Aeronautical Engineering, University of the Witwatersrand, Johannesburg, South Africa

A R T I C L E   I N F O

Article history:
Received 17 February 2014
Received in revised form 15 May 2014
Accepted 17 June 2014
Available online 9 July 2014

Keywords:
A. Polymer Matrix Composites (PMCs)
B. Mechanical properties
B. Stress transfer
D. Mechanical testing
Hybrid composites

A B S T R A C T

Nano-strengthened hybrid GRP composites were mechanically characterized for different multiwalled carbon nanotube (MWCNT) mass fractions of 0.1 wt%, 0.5 wt% and 1 wt% based on a 32 wt% glass fiber mass fraction. The selection of fabrication parameters for hybrid composites was based on tensile, flexural, and impact property results obtained from plain glass reinforced fiber composites (GRPs) by varying fiber mass fractions of 24 wt%, 32 wt% and 40 wt%. Results obtained indicated the 32 wt% as being the optimum mass fraction for the fabrication of GRP hybrid composite. For hybridization, functionalized multiwalled carbon nanotubes were selected as a secondary reinforcement and the optimum functionalization parameters were determined by considering three different functionalization times of 6 h, 24 h and 48 h respectively. The optimum functionalization time was then selected based on morphological characterization of functionalized MWCNTs which was performed using Raman, TEM and FTIR techniques. Based on the results obtained, the 24 h functionalization period on MWCNTs with nitric acid was found to be the most suitable. The final hybrid was then fabricated based on 32 wt% fiber fraction however with three different MWCNTs mass fractions for further characterization. The results obtained show that the nano-strengthened GRP hybrid composites reinforced with 0.5 wt% functionalized MWCNTs exhibit substantially better properties than those of plain GRP, 0.1 wt% and 1 wt% of functionalized MWCNT composites. At higher fiber mass fraction of 40%, the load transfer efficiency was reduced resulting in poor mechanical properties and similar behavior was also observed for hybrid composite with 1 wt% of CNTs. This anomalous behavior can be attributed to the poor quality of specimens due to fiber agglomerations in some places due to higher mass fraction which caused poor penetration of resin into the fiber mat resulting in inefficient load transfer.

1. Introduction

A common fiber reinforced composites (FRPs) consist of a polymer matrix embedded with fibers such as glass, aramid, and carbon [1] and has taken a central role in engineering design for the last 20–30 years due to their ease in processing, tailorable properties and weight savings compared to metal alloys [2]. Generally, composite properties depend on the properties of the individual constituents, geometry and the distribution of individual constituents [3,4].

Glass reinforced composite (GRP) is one of the subset of the composite groups, used in number of engineering applications, replacing the most commonly used materials such as steel. Their importance is mostly realized in aviation, aerospace, automobile, ship building, submarines, nuclear and chemical facilities with extremely harsh environmental conditions. GRP composites can be categorized as either continuous or discontinuous based on the fiber reinforcements. The mechanical properties of GRP composites are designed to be superior to those of their constituent materials and depend on the constituents properties, geometry and distribution [5]. However a common shortcoming with GRP composite is the failure in matrix-rich inter-laminar regions where the stress transfer between load-bearing fibers occurs. Even for the higher volume fraction (60%) of fibers, the local matrix-rich regions persist (refer Fig. 1) and are of critical concern in commercial applications where the failure at the inter-laminar regions can be catastrophic. As a result, researchers are focusing on investigating the nano-strengthened-GRP hybrid composite systems where, the matrix is strengthened with the second reinforcement in the form of nano-particles, which is expected to improve both the interlaminar regions and the properties [6,7]. According to Kickelbick [8],

---

* Corresponding author. Fax: +27 (0) 11 717 7049.
E-mail address: jacob.muthu@wits.ac.za (J. Muthu).

http://dx.doi.org/10.1016/j.compositesb.2014.06.012
1359-8368/© 2014 Elsevier Ltd. All rights reserved.

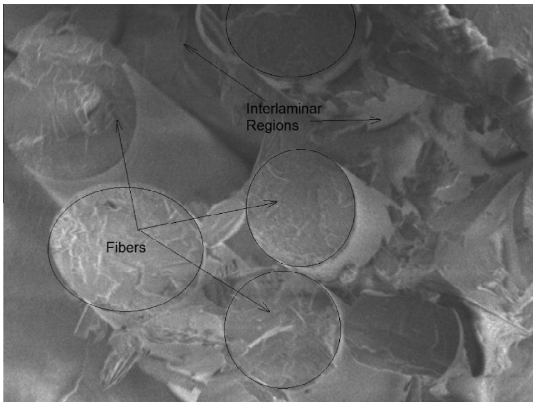

Fig. 1. Inter-laminar region in a composite specimen.

decreasing the size of the inorganic units to the same level as the organic building blocks could lead to more homogeneous materials that allow a further fine tuning of material properties at molecular and nanoscale level.

A composite is termed “hybrid” if two or more different reinforcements are used in a composite system and are generally termed as multi-scale reinforced composites where the nano-particles are incorporated into the matrix system to increase the stiffness, strength, and toughness. Other than attaining higher order properties, the hybrid composites offer benefits such as low cost, better strength to weight ratio, post-failure behavior and fatigue performance that lead to most material engineers tailoring the hybrid materials to their exact structural requirements [9,10].

Since the discovery of carbon nanotubes (CNTs) by Iijima [11] in 1991, they have received much attention in wide range of applications such as nanoelectronics [12], gas and energy storage [13], nanowires [14], and nanocomposites [15]. Basically, CNTs have the arrangement of hexagonally shaped carbon atoms (graphene) rolled into tiny tubes having diameters ranging from a few angstroms to tens of nanometers and can have lengths of up to several centimeters. CNTs can be viewed as a hollow coaxial cylinder of graphite layers and are generally classified as single-walled CNTs (SWCNTs), double-walled CNTs (DWCNTs), and multiwalled CNTs (MWCNTs). CNTs exhibit excellent mechanical, electrical, thermal, and magnetic properties [16]. The exact magnitude of these properties depends on the diameter and chirality of the nanotubes and whether they are single-walled, double-walled, or multi-walled. The combination of these physical and mechanical properties make CNTs highly desirable candidates as reinforcements for both nano and hybrid composite materials.

Though the hybrid composites can be fabricated using various combinations of the reinforcements, the nano hybrid processing is quite simple and cheaper as compared to adding two different macro-size fillers into the hybrid systems. The general procedure for fabricating hybrid composites is that the matrix will be strengthened by nano-particles prior to blending with the fiber. In recent years, several studies have been conducted on manufacturing GRP composites strengthened with carbon nanotubes (CNTs). However the practical challenges concerning their fabrication still remain and need to be addressed before realizing the full potential of CNTs strengthened multiscale hybrid composites [17].

These challenges can be summarized as [18].

- An appropriate dispersion of the CNTs into the polymer matrix.
- A sufficient interfacial bonding between polymer matrix and nano-fillers.
- An improved interlaminar region.

Various dispersion methods of CNTs into polymer matrices such as stirring and sonication have been reported in the literature. Most of these methods are either limited in capacity or not capable of separating the agglomerates into individual nanotubes. One common technique for dispersing CNTs into the polymer matrices is sonication. However, the reduction in vibrational energy with increasing distance from the sonotrode limits the usage of sonication method only to small batches. An additional detrimental effect of this method is the rupture of the CNTs caused by the local energy input resulting in reduction of the effective tube length [19].

Secondly, the factor affecting the strengthening of polymers using CNTs is the interfacial adhesion between the CNTs and the polymer matrix. The interfacial adhesion plays an important role in load transfer from the matrix to CNTs and this is vital for the exploitation of CNTs potential as a secondary reinforcement for hybrid composites. The interfacial adhesion can be improved by chemical functionalization of the nanotube surface [20]. There are several approaches for functionalization of CNTs including defect functionalization, covalent functionalization, and noncovalent functionalization. Moreover, it has been pointed out that the introduction of functional groups (COOH and OH groups) on the CNTs surface reduces CNTs agglomeration and improve dispersion in both polar and no-polar solvents [21]. Recent research reports [22,23] have indicated that the addition of functional groups on the CNTs surface can improve the dispersion of CNTs which acts as a principal driver in getting the desired optimum properties. Work of similar nature [24] has also shown that the functionalization has improved the interfacial bonding strength between the nanotubes and the polymer matrix.

Based on the above observations, the objective of this study has been defined as the characterization of the GRP fiber composites hybridized with functionalized multiwall carbon nanotubes. We start with obtaining an optimum glass fiber mass fraction for the GRP composites. Then the chemical functionalization of CNTs for different period of times to get the optimum functionalization time is detailed. Finally, the fabrication of the hybrid composites using the optimum glass fiber mass fraction along with the different weight fraction of CNTs and the characterization results are presented.

2. Experimental

2.1. Materials

The multi-wall carbon nanotubes (MWCNT) supplied by SABI NANO of South Africa were used as the filler for strengthening the polymer matrix. The MWCNT has the diameter in the range of 30–35 nm and the average length of 50 μm with greater than 90% purity. The range of relative density is 1.7–2.1 mg/cm^3. The MWCNTs have entangled cotton like fiber structure and shown in Fig. 2.

The Luperox curing agent and the polyester resin (CoREZYN VE 8300) matrix were supplied by NCS Resins South Africa. The density of the polymer at room temperature is 1155 mg/cm^3. The chopped strand mats (CSM 450 and CSM 300) supplied by Fibre Wound (Pty) Ltd, South Africa (Fig. 3) were used as the reinforcements. The C-glass tissue fiber mats were also used to form the outer layers of the composite specimens. NCS Waxol was used to polish the mold surface to ensure a clean surface before lamination. A MR8 release agent was applied on the steel mold for the easy removal of the finished components. All reagents used were of analytical grade.

2.2. Functionalization of MWCNTs

The MWCNTs were functionalized before blending with the polymer. The as-received multi-wall carbon nanotubes were func-

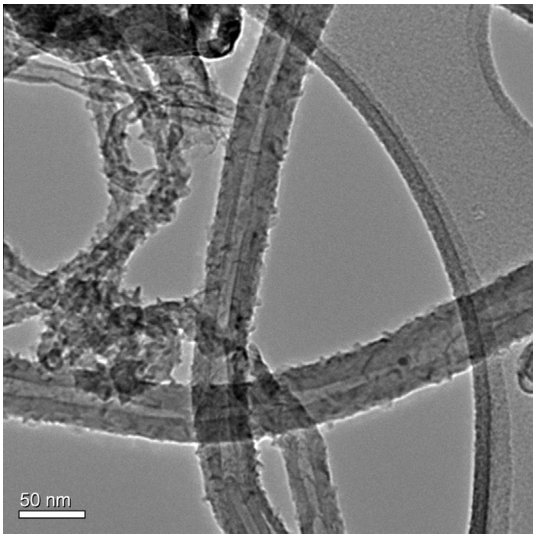

Fig. 2. TEM image of MWCNT.

tionalized with nitric acid (HNO_3) by oxidation method under refluxing condition. First 2 g of MWCNTs were added into a beaker with 300 mL of 55% concentrated nitric acid. The mixture was then refluxed at 100 ° C and then allowed to cool to room temperature. They were then washed with deionized water until neutral pH and vacuum filtered using a 3 μm porosity paper. The filtered functionalized MWCNTs were dried for an hour at 100 °C. Three different functionalization times of 6 h, 24 h and 48 h were selected to obtain the optimum functionalization time. In order to confirm, whether the similar degree of functionalization was obtained, functionalized CNTs were characterized using TEM, FTIR, Raman spectrum and thermogravimetric analysis.

2.3. GRP and GRP hybrid composite fabrication procedure

The composite specimens were fabricated using a contact molding procedure in general accordance to the requirements of ISO 1268-2:2001 except that the specimens were subjected to uniform pressure on the open surface to ensure a uniform thickness throughout the entire length of the test specimens. The composite specimens were manufactured using glass fiber in the form of chopped strand mat (CSM) as a reinforcement and the unsaturated polyvinyl ester resin (CoREZYN VE 8300) as matrix.

The GRP composite specimens were fabricated for three different glass fiber mass fractions of 24%, 32%, 40% as recommended by ISO-1268-2 for chopped strand mats. The corresponding resin content was determined using the following formula which was taken from the ASTM standard of ISO-1268-2.

$$m_2 = m_1 \frac{(100 - m_1 - w_g)}{w_g} K$$

where

m_1 = mass of glass in grams,
m_2 = mass of resin required in grams,
w_g = glass fiber content desired in the laminate expressed as a percentage of the total mass,
K = constant representing 20% of excess resin lost through spills and absorption of by rollers.

Before starting the lamination procedure, the steel mold was cleaned using acetone followed by drying using a dry cloth. As part of the priming procedure, a thin film of MR8 release agent was applied on the mold surface. Then, 1.5 kg of CoREZYN VE8300 polymer matrix was mixed with 0.5 g of Luperox catalyst as per the process manual and the solution was stirred well. With the aid of a roller brush, the first thin coat of resin was applied on the mold followed by the barrier C-glass tissue fiber which acts as a corrosion barrier in real product applications. After placing the C-glass fiber, the steel roller brush was used to apply pressure gently against the laminate. The process was repeated until alternative layers of CSM450 and CSM300 fiber mats were added to achieve the desired fiber mass fraction (Fig. 4) and then followed by a final layer of C-glass as an outer corrosion barrier layer.

Finally a mixture of 500 g of resin, 0.2 g of Luperox catalyst and 2 drops of wax-in-styrene (NCS Waxol) was applied to all the sides of the laminate. The completed laminate was later subjected to uniform pressure with a flat plate to ensure an uniform thickness throughout the specimen before curing at 60 °C for 24 h in a vacuum oven. The similar procedure was followed for 24%, 32% and 40% mass fraction of laminates respectively. The laminates were stored inside a desiccator for further analysis.

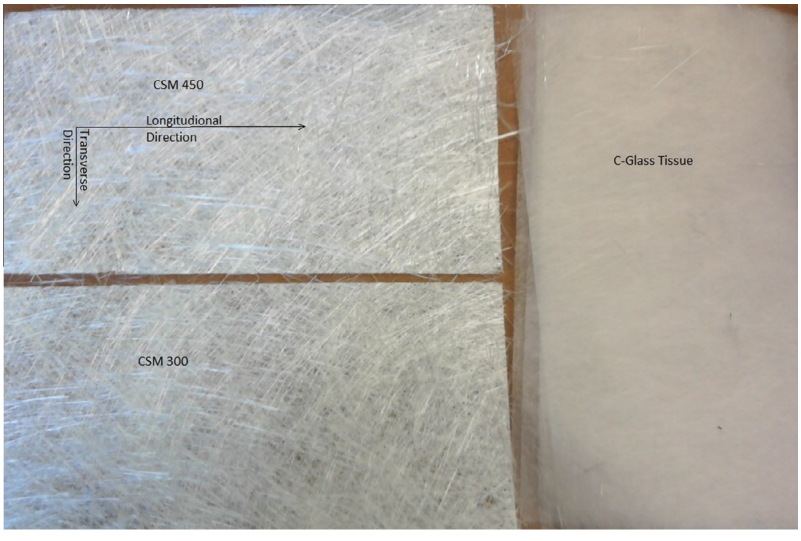

Fig. 3. CSM 450, CSM 300 and C-glass tissue fiber mats.

The same procedure was followed for manufacturing hybrid composites except that the polymer matrix was mixed with three different weight fractions (0.1 wt%, 0.5 wt% and 1 wt%) of functionalized MWCNTs. Fig. 5 shows the different stages of blending the MWCNTs with the matrix. However the hybrid composites were not fabricated for all three fiber mass fractions. Before fabricating the hybrid composites, the GRP composites were tested and the results were analyzed. Based on the results, an optimum fiber mass fraction was selected for fabricating the nano-strengthened hybrid composite specimens.

3. Mechanical characterization

3.1. Testing procedure

The fabricated GRP and hybrid composite specimens were tested to determine the mechanical properties. The Tensile, Impact and Flexural specimens were fabricated based on ASTM $D638-08:2010$, ASTM $D256-06a:2010$ and ASTM $D790-07:2010$ respectively. The tensile specimens are shown in Fig. 6. As per the ASTM standard, the thickness of the tensile testing specimen was kept at 3.2 mm (Fig. 6). The tensile test was carried out using a Lloyd MX100 tensile testing machine at a cross head speed of 2 mm/min according to the DIN $EN527.1/2$ standard and the results were used to obtain the tensile strength and the Elastic modulus. The flexural properties were determined using the same machine by carrying out three-point bending tests as per the ISO 178 standard. The flexural test specimens were fabricated with the thickness to span ratio of 1:16 and the tests were conducted at the cross head speed of 2 mm/min. Notched impact tests were carried out as per the ISO 179-1 standard on a Zwick impact pendulum.

3.2. Tensile testing procedure

A load cell of 50 kN was used to conduct the tensile testing. Prior to testing, the specimen s thickness and width were measured. The alignment and adjustment of the test specimen with respect to the loading axis of the testing machine is very important so that the experimental results can be compared with the theoretical work and the prototype experimental results can be extended to practical application. Hence the special care has been taken while mounting the specimens with the testing machine. The experimental data were recorded using Lloyd MX100K built-in encoder. An external extensometer was used to record the linear portion (Elastic region) of the data. For tensile testing, the test specimens were cut along the longitudinal direction of the laminates.

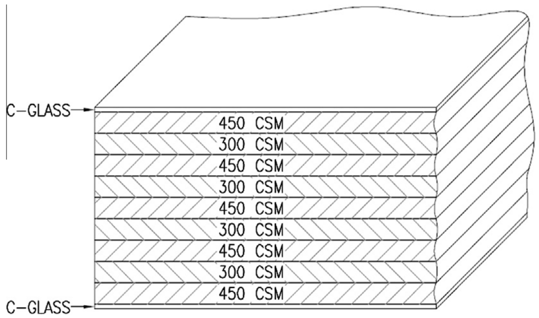

Fig. 4. A schematic of the lamination procedure.

3.3. Flexural testing procedure

The flexural testing was performed using the same Lloyd testing machine of 50 kN load cell using the 3-point flexural testing attachment. The built in encoder was used to acquire the required data. The distance between the specimen supports was 63 mm. The test specimens were cut along the longitudinal direction only.

3.4. Impact testing procedure

The Izod impact testing method was used to determine the impact strength of the fabricated composite specimens. An Avery pendulum impact testing machine with static dial arm, which can manually be moved and positioned prior to testing at 4.2 J mark, was used to perform the impact testing. During the experiment, the pendulum was manually released on to the mounted specimen and the dial gauge readings were recorded to obtain the energy required to break the specimen. With no specimen, the dynamic dial arm moves up to zero indicating that no energy was absorbed. The measuring range of the testing machine is from 0 to 4.2 J with the resolution of 0.025 J. The test specimens were cut along the longitudinal direction only.

3.5. Morphological characterization

Morphological characterization of the MWCNTs was carried out using a Transmission Electron Microscopy (TEM) of make Tecnai G2 TEM at 12 kV. Electron microscopy images were taken using the FEI Quanta 400F Environmental scanning electron microscopy machine. The scans were done in high vacuum at 2 kV in secondary electron imaging (SEI) mode. Before scanning, the fracture surface of the specimens was coated with a thin layer of carbon in an EMITECH K950X evaporator. The samples were then coated with a 15 nm layer of gold–palladium (Au/Pd) on a ratio of (60:40) in an EMITECH K550X sputter coater and then attached to 1 cm diameter stubs with DAG 580 colloidal graphite. The thermal stability of the as-received MWCNTs and the functionalized MWCNT s was determined using a Perkin-Elmer-Pyris thermo-gravimetric analyzer under an air flow of 20 mL/min. Raman spectra were recorded at ambient temperature on a Jobin–Yvon T6400 micro-Raman spectrometer using a tunable Physics dye laser with a 636.4 nm excitation source.

4. Results and discussion

4.1. Mechanical characterization of the GRP composites

A number of GRP composite specimens were tested to obtain their mechanical properties. The specimens were fabricated with the fiber mass fraction of 24%, 32% and 40% respectively. The tensile testing specimens were cut along the longitudinal direction of the fabricated composite panes.

4.1.1. Tensile testing

The test specimens were carefully aligned with the testing machine loading axis and the data were recorded using the built-in data acquisition system. Fig. 7 shows the stress–strain curve of the plain GRP tensile specimens.

As expected, the tensile strength and the young modulus increase with the increase in fiber mass fraction of 24–32 wt% (Figs. 8 and 9). The increase in the tensile properties is primarily attributed to the reinforcing effect of fibers which permits uniform load transfer from the polymer matrix to the reinforced fibers.

Fig. 10 shows a Scanning Electron Micrograph (SEM) of 32% mass fraction of GRP composite tensile test specimen fracture sur-

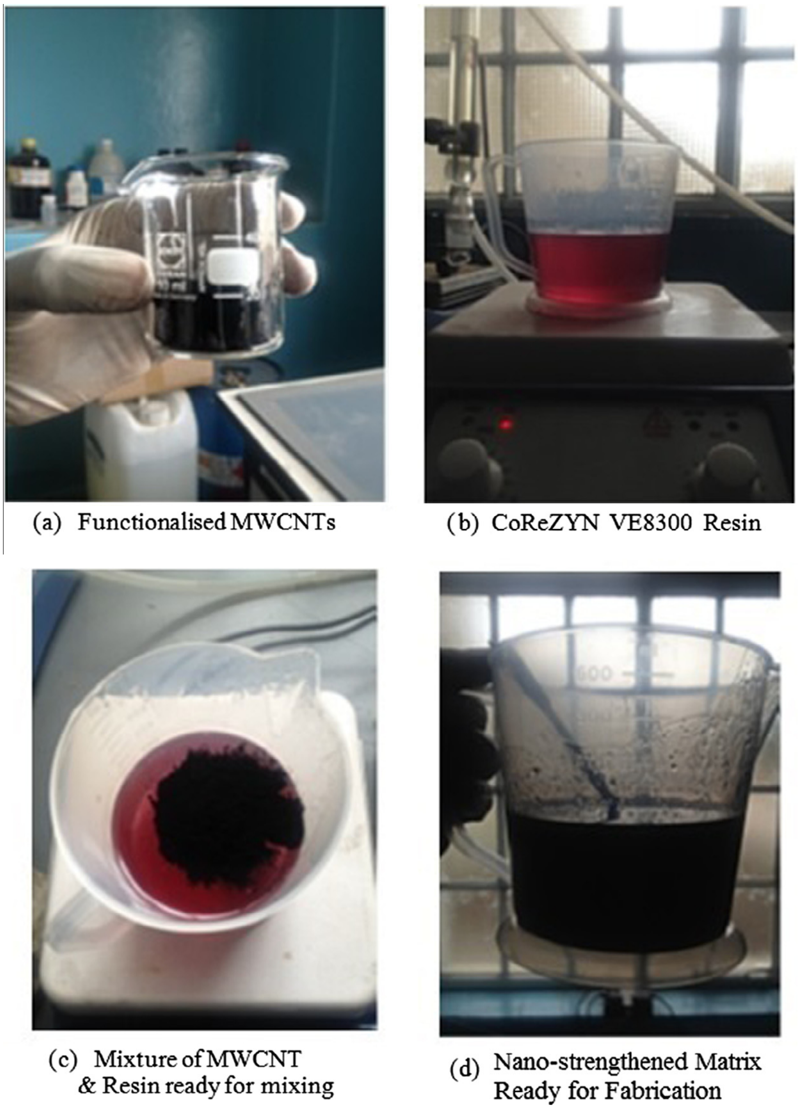

Fig. 5. Different stages of strengthening the polymer matrix using MWCNTs.

Fig. 6. Tensile testing specimens.

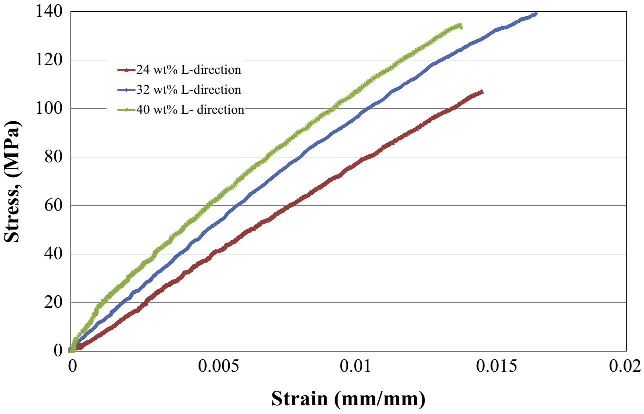

Fig. 7. Stress–strain curve of the GRP composite specimens.

face. It can be seen from the micrograph that the load transfer has been taken place from the matrix to the fiber which can be confirmed by less fibers pull out and more broken fibers. This is a broad indication of better bonding between fibers and the matrix.

However, the influence of fiber volume fraction on the mechanical properties has started to diminish as the fiber content is increased from 32% to 40% mass fraction. The average value of the tensile strength and young modulus of the GRP composite specimens with 32% fiber mass fraction along longitudinal direction are 138 MPa and 9.5 GPa respectively. However, the specimens with 40% mass fraction cut along the same direction did not show appreciable increase in the tensile strength and Young modulus and the obtained values are 134 MPa and 9.8 GPa respectively. The anomalous behavior can be attributed to both fiber agglomerations in some places due to higher mass fraction and poor penetration of matrix into the fiber mat which led to fibers touching to each other. Fig. 11 presents the micrograph of the fracture surface of the composite made with 40% fiber mass content. Poor penetration of resin into the fiber mat and the fiber agglomeration are readily seen. This explains the reduction in mechanical properties of the composites when the fiber mass content was increased from 32% to 40%.

4.1.2. Flexural and impact testing

The three point bending tests were performed on the GRP composite specimens. Fig. 12 shows the flexural strength and modulus of the composites for the fiber mass fraction of 24%, 32% and 40% respectively. The flexural properties increase when the fiber content increased from 24 wt% to 32 wt%. This is intuitive. However, the flexural properties did not show appreciable increase when the fiber mass fraction increased to 40%. It is substantially lower than one would expect. This anomalous behavior may be attributed to the agglomeration of fibers resulting in fiber to fiber interaction (fibers touching to each other) and poor fiber bonding with the matrix as discussed before.

Experimental determination of fracture toughness was performed on notched GRP composite specimens and is shown in Fig. 13. The fracture toughness values of the composite specimens with 24 wt%, 32 wt% and 40 wt% fiber mass fraction are shown in Fig. 14. The results show that the fracture toughness values increases with the increase in fiber mass fraction from 24% to 32%. Moreover the similar trend was observed as the fiber mass fraction were increased to higher values.

As can be seen from the results, the mechanical properties of the GRP composites increase for the substantial increase in fiber mass fraction to 32% and started to decrease for the higher values. The reason for decrease in properties for higher fiber mass may be attributed to the agglomeration of fibers and insufficient bonding between fiber and matrix. Based on the above observations, the GRP hybrid composites (HGRP) are fabricated using the (optimum) fiber mass fraction of 32% for characterizing the effect of carbon nano-particles at the interlaminar regions.

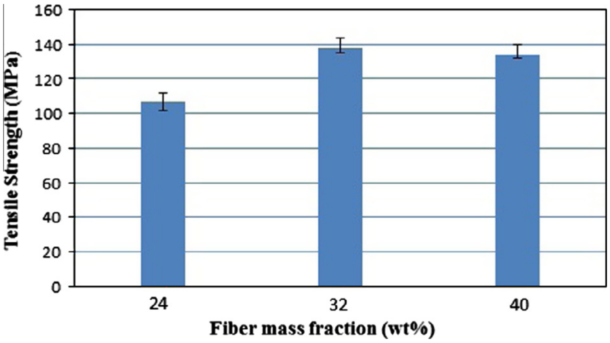

Fig. 8. Tensile strength of the GRP composite specimens.

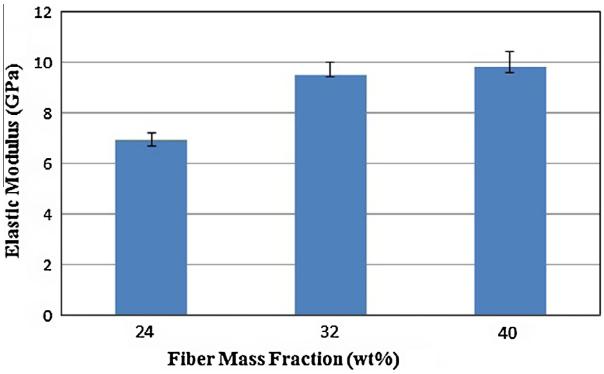

Fig. 9. Elastic modulus of the GRP composite specimens.

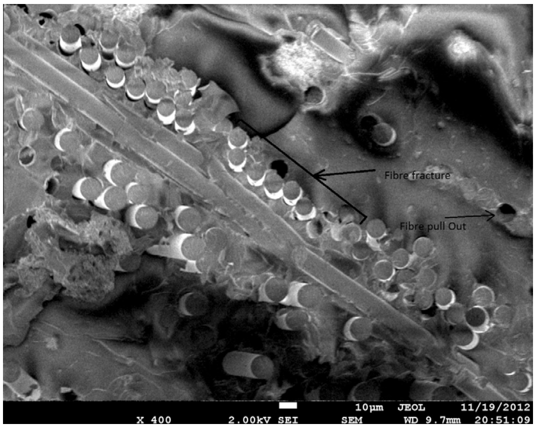

Fig. 10. SEM micrograph of 32 wt% GRP composite.

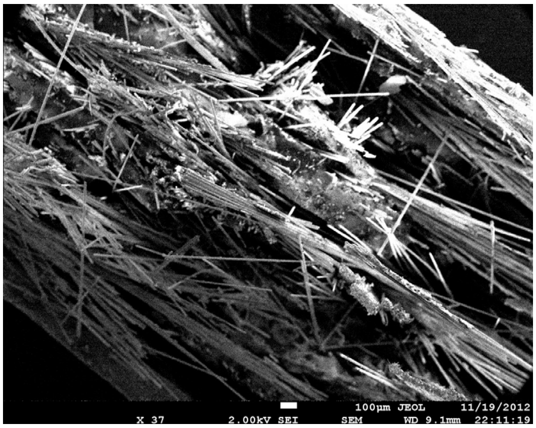

Fig. 11. SEM micrograph of 40 wt% GRP composite.

4.2. Functionalization of MWCNTs

The performance of CNTs as an additional reinforcement in hybrid composites depends on the dispersion of CNTs into the matrix and the interfacial interaction between the matrix and the CNTs at the interlaminar regions. As discussed before, modifying the CNT surface properties by attaching the functional groups (OH and COOH) can achieve the desired results. The amount of

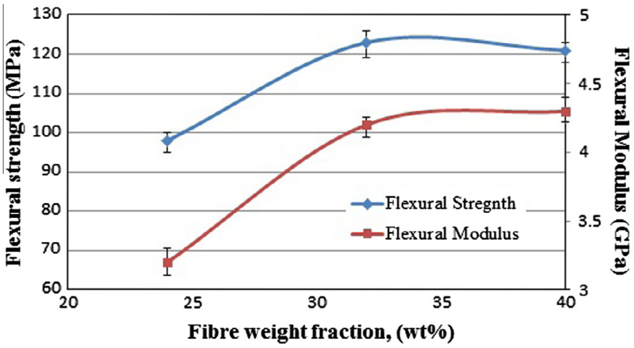

Fig. 12. Flexural properties GRP composites.

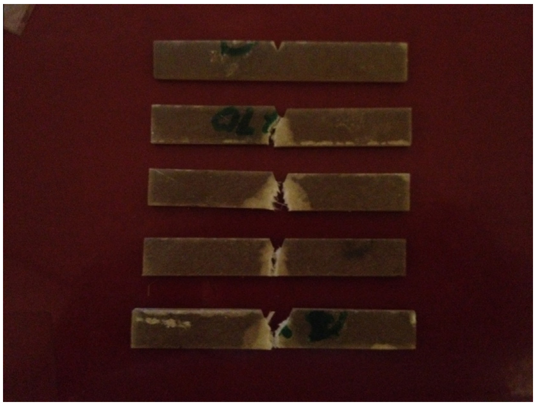

Fig. 13. Impact testing specimen.

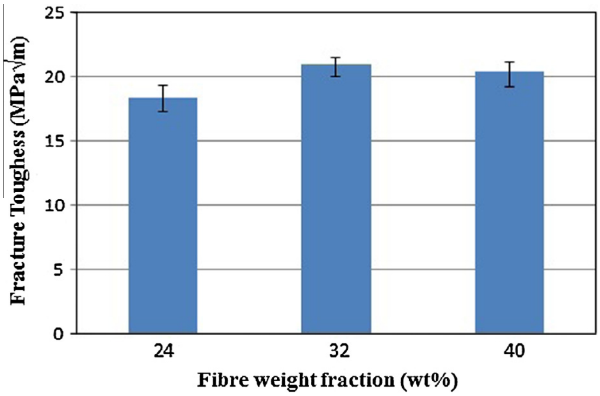

Fig. 14. Fracture toughness of GRP composites.

the attached functional group is believed to be proportional to the functionalization periods. However the structural changes in CNTs resulting from the functionalization could be detrimental to the CNTs desire properties and very limited details are available to provide consensus on the factors affecting the functionalization.

Hence, for the current analysis, focus has been directed towards understanding the effect of functionalization periods on the CNTs surface. Three functionalization time levels of 6hours, 12 h and 48 h were selected respectively. As described before, 2 g of the as-received MWCNT material was treated with 55% concentrated nitric acid for three different time periods. The mixture was refluxed at 100 °C, then diluted and cooled before investigating the optimum functionalization time. The chemical treatment leads to removal of catalyst from the CNTs, opened the tubes ends and formation of functional groups at defected sites along the side walls. The final products (MWCNTs) were decorated with various oxygen-containing groups, which were then analyzed to determine the quantity of the functional group and the quality of the CNTs.

4.2.1. Transmission Electron Microscopy (TEM)

TEM was used to study the possible morphological changes on MWCNT specimens due to the chemical functionalization.

Fig. 15(a) shows the TEM image of the pristine CNT. Before functionalization the CNT tube structure are not clear and the traces of the catalyst and the amorphous carbon materials remains on the nanotubes. The TEM image of MWCNTs functionalized for 24 h is shown in Fig. 15(b). After functionalization, the MWCNT walls are clean and no changes in the morphology are detected. Moreover, the graphite structure of the MWCNTs was not disturbed and at the same time the functionalization treatment has removed the catalyst and the amorphous carbon from the carbon nanotubes. However, Fig. 15(c) which is the TEM image of MWCNTs functionalized for 48 h, appears to be exfoliated and the tube structure were damaged due to the long duration of functionalization. It was also clear that the aggressive acid functionalization for 48 h, has destroyed the tube structure and shorten the length, which could affect the CNTs properties as a strengthening reinforcements.

4.2.2. FTIR, Raman and thermogravimetric analysis (TGA)

Raman scattering is a powerful technique to characterize and probe the structure–property relationship in both pristine and functionalized CNTs. Fig. 16 shows typical Raman spectrum of pristine, 24 h and 48 h functionalized MWCNTs. Two Raman peaks at 1350 cm-1 (D band) and at 1600 cm-1 (G band) were observed which has been attributed to disorder in the hexagonal frame work of the nanotube walls. The ratio of the intensity of the G band to that of the D band (I_G/I_D ratio) shows the crystalline structure and the purity of the carbon nanotubes. Though the peaks in the spectra fairly look similar to each other, the ratio of G to D values can reveal the disorder in the carbon nanotube structure. The higher the ratio, the more the material is crystalline. When the functional groups are attached to the side walls of the carbon nanotubes which reduce the crystallinity of the CNTs. Thus, one way of checking the degree of functionalization is by measuring the Raman spectrum and comparing the I_G/I_D ratio of the pristine with the functionalized CNTs. The calculated I_G/I_D ratios were 1.2, 0.9 and 0.8 for pristine, 24 h and 48 functionalized MWCNTs respectively. It was noticed that the I_G/I_D ratio decreases with increase in functionalization times. This result shows that MWCNTs were functionalized and at the same time reveals that the degree of functionalization depends on the time of functionalization.

To obtain further information, TGA was performed with samples from the three functionalized time periods. Figs. 17 and 18 show the results of the thermogravimetric analysis (TGA), of the pristine and the functionalized MWCNTs for 6, 24 and 48 h. The pristine MWCNTs show a residual mass of 10% consistent with the supplier data of 90% purity MWCNT. After functionalization, the residual mass decreased to greater than 4%. This behavior reflects that the functionalization helped in purifying the CNTs. The decomposition temperature of MWCNTs started to decrease as the functionalization period increased from 6 to 48 h. The decomposition temperature of the pristine CNTs was 640 °C and as the functionalization time increased to 48 h, the decomposition of MWCNTs reduced to 590 °C and can be seen in Fig. 17.

The above results were also consistent with the FTIR data which shows that the extent of functionalization increased with time of functionalization. Fig. 19 shows the FTIR spectra of as-received and treated MWCNTs. A typical FTIR spectrum of MWCNTs functionalized for 24 h shows two peaks at 1730 cm^{-1} and

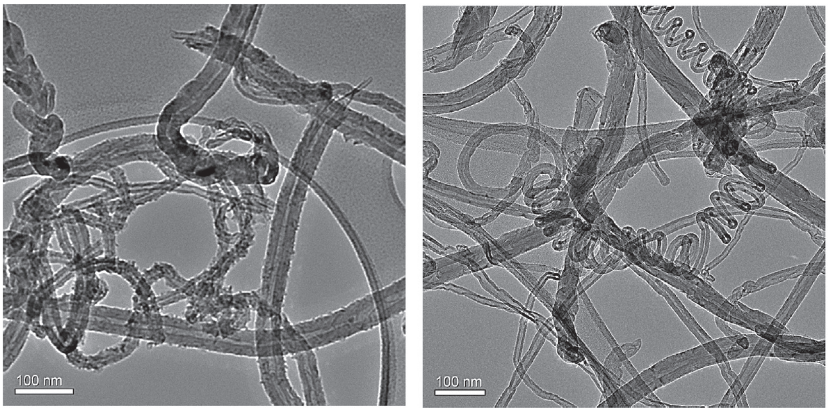

(a) Pristine MWCNTs (b) MWCNTs Functionalized for 24 hours

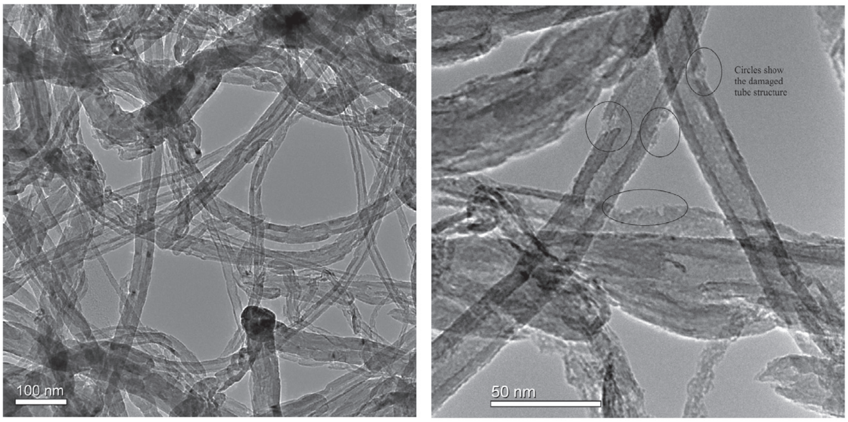

(c) MWCNTs Functionalized for 48 hours (d) MWCNTs Functionalized for 48 hours with damaged tube structure

Fig. 15. TEM image of pristine and functionalized MWCNTs.

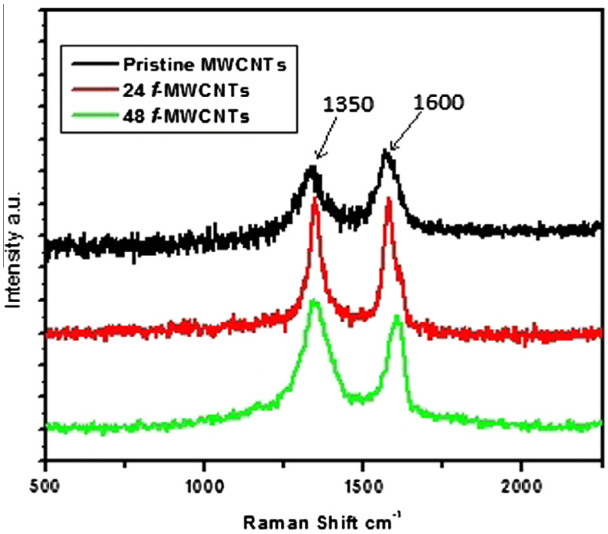

Fig. 16. Raman spectrum of the pristine and functionalized MWCNTs.

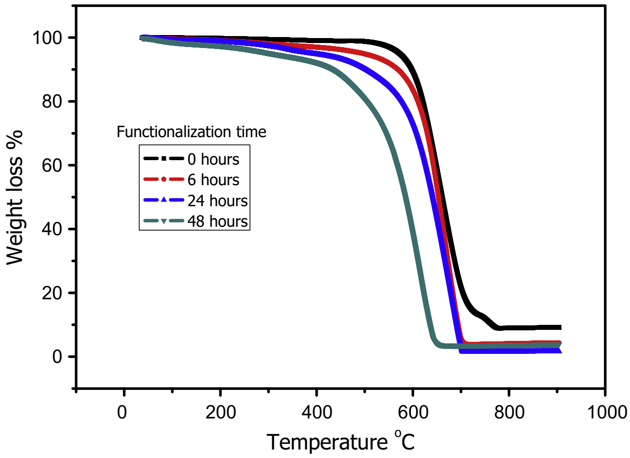

Fig. 17. TGA of pristine and functionalized MWCNTs.

1566 cm^{-1}. These are normally assigned to the C=O stretch vibration in the —COOH group, which means that the nitric acid treatment indeed, attached —C=O groups to the side walls of the MWCNTs.

Fig. 20 shows the functionalized MWCNTs dispersed in water. Sample "A" refers pristine MWCNT, "B" refers CNT functionalized for 6 h and "C" refers Sample treated for 24 h. The sample treated for 24 h remains dispersed in water for a month. However the pristine MWCNTs settle down quickly. The samples functionalized for 24 h were tested with other solvents. The resulting distribution of MWCNTs shows the similar behavior.

Based on the above results, it has been confirmed that the treatment of MWCNTs with concentrated nitric acid achieves the required functionalization by attaching OH and COOH groups on the side walls of the MWCNTs. Extended period of functionalization results in the weakening of the MWCNTs and

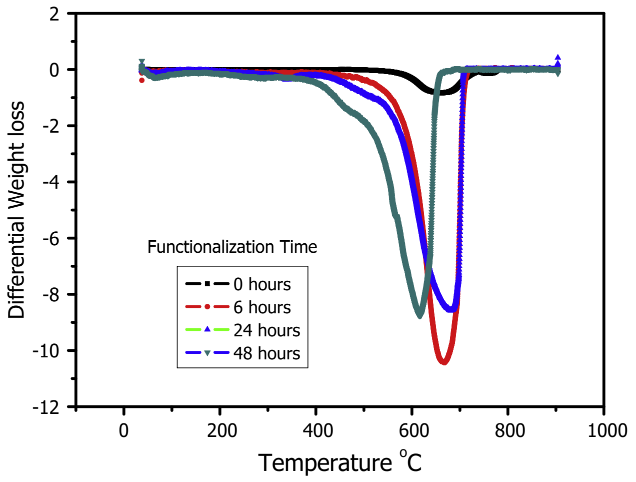

Fig. 18. TGA of differential weight to temperature of pristine and functionalized MWCNTs.

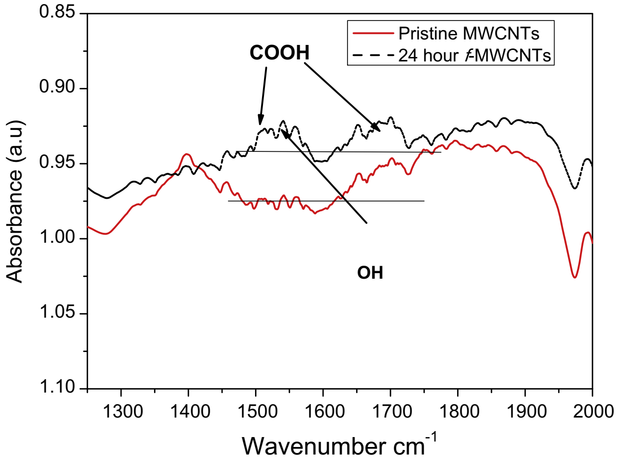

Fig. 19. FTIR results for pristine and functionalized MWCNTs.

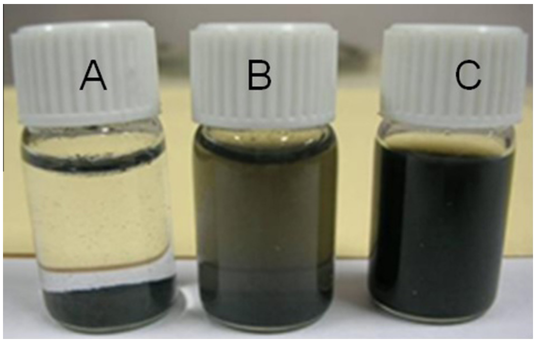

Fig. 20. Functionalized MWCNTs dispersed in water.

can be seen from TEM data (Fig. 15) and thermal stability results (Fig. 17). Hence it has been concluded that the 24 h functionalization was the optimum functionalization period for the given MWCNTs.

4.3. GRP-hybrid composites

Using the above experimental results, the parameters for fabricating the hybrid composites were chosen as 32 wt% of glass fiber content with the MWCNTs functionalized for 24 h. The nano-strengthened hybrid composite specimens were fabricated using the similar procedure used for making GRP composites. An appropriate amount of polymer matrix were mixed with three different functionalized MWCNTs weight fraction of 0.1 wt%, 0.5 wt% and 1 wt% respectively. The mixture was vigorously stirred approximately for an hour before adding the catalyst. The lamination procedure was carried out as explained in GRP composite fabrication procedure. Fig. 21 shows nano-strengthened hybrid composite tensile test specimen.

4.3.1. Mechanical characterization of the GRP-hybrid composites

The GRP hybrid composites were tested to obtain their mechanical properties. Figs. 22 and 23 show the average tensile strength and Young Modulus of the hybrid composite specimens respectively.

The effect of hybridization can be seen from the results. The average tensile strength and the young modulus values for the 32% glass fiber mass fraction composites increase with the increase in CNT weight fraction from 0.1 wt% to 0.5 wt%. The significant increase in the tensile properties is primarily attributed to the reinforcing effect of MWCNTs which strengthens the matrix. The tensile strength of the hybrid composites with 0.1 wt% of CNT has shown improvement as compared to the plain GRP composite specimens. The average tensile strength of the 0.1 wt% CNT strengthened hybrid composite gives the value of 142 MPa which is 3% improvement than the GRP plain composites. Similar behavior has also been seen as the CNT weight fraction increased from 0.1 wt% to 0.5 wt%. The average tensile strength of the 0.5 wt% CNT strengthened hybrid composite gives the value of 152 MPa which is closely 10% increase than the GRP composite.

Mainly two factors can explain the improved mechanical properties of the hybrid composites. Jacob and Paskaramoorthy [23] showed that the improved interfacial load (stress) transfer can be obtained by the uniform distribution of the functionalized carbon nanotubes within the matrix and the formation of matrix coating around the nanotubes. This is one of the reasons for the improved tensile properties of hybrids when compared with plain specimens. During lamination, the functionalized CNTs tend to aggregate around the glass fibers and the polymerization promotes the cross linking reaction between the functional groups of the CNTs and the polymer matrix on one hand and to the sizing of the glass fibers which also contain the epoxy groups on the other hand. These cross links increase the interfacial strength which could explain the improved mechanical properties. Fig. 24 shows a SEM image of 0.5 wt% CNTs hybrid composite fractured surface and it is apparent that the cross linked CNTs with the polymer matrix were attached to the surface of the glass fiber. From the above observation, it can be said that the functionalized CNT's were an effective strengthening mechanism for the hybrid composites.

Moreover, with the low concentrations, the functionalized CNTs can be homogeneously dispersed with the polymer matrix and at the same time reduced self interaction among themselves leads to improved mechanical reinforcement. The influence of CNTs weight fraction on the hybrid composite properties can also be seen with the given results. Though the mechanical properties increases with increase in CNT weight fraction, the similar trend is not continuing for the large amount of functionalized CNTs, say 1 wt%. The anomalous behavior can be attributed to the CNT agglomerations which acts as a stress riser along the load transfer path.

Fig. 25 shows the flexural properties of the GRP-hybrid composites. The flexural modulus in each case was determined by measuring the slope in the linear region and the flexural strength is the maximum stress in the corresponding stress–strain curve. It can be seen that the similar trend can be observed for the flexural

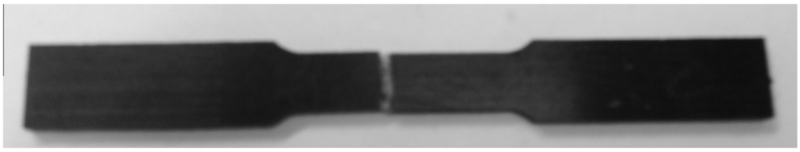

Fig. 21. Nano-strengthened hybrid composite tensile test specimen.

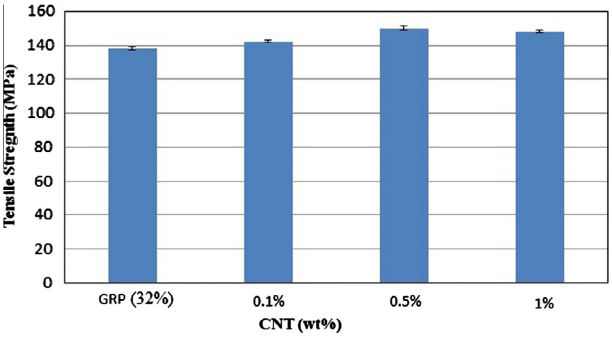

Fig. 22. Tensile strength of hybrid composites.

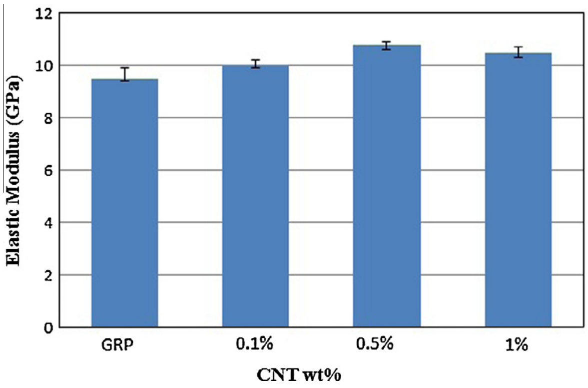

Fig. 23. Elastic modulus of hybrid composites.

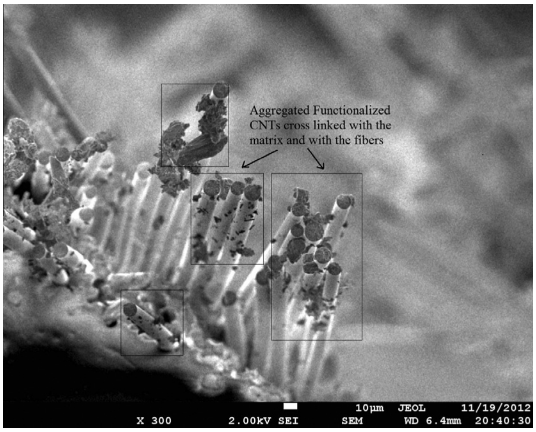

Fig. 24. CNTs cross linked with both the polymer matrix and the glass fibers.

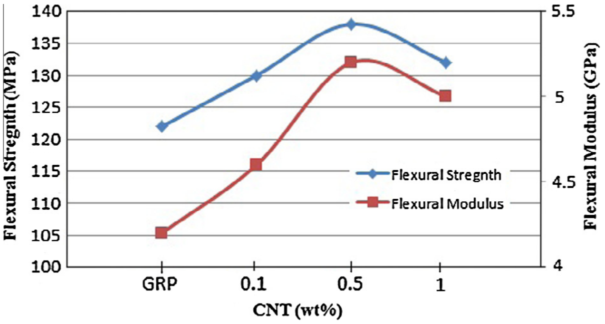

Fig. 25. Flexural properties GRP composites.

Fig. 26. Nano-strengthened hybrid composite impact specimens.

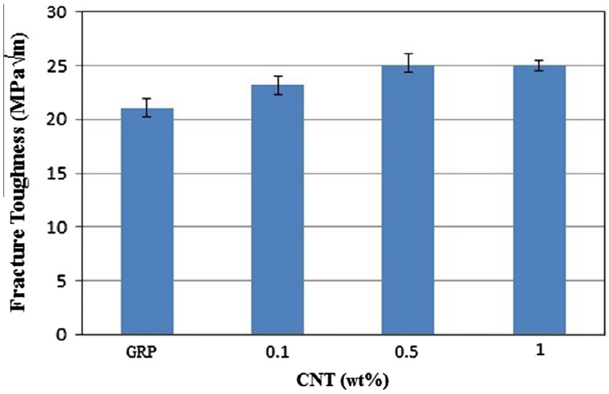

Fig. 27. Fracture toughness of GRP composites.

properties as compared with tensile properties. As shown in the figure, the flexural strength and the flexural modulus of hybridized GRP-composites were improved to approximately 13% and 23% respectively for the addition of 0.5 wt% of functionalized CNTs. However, for the addition of 1 wt% of functionalized CNT, the flexural properties does not show appreciable increase in their values.

The plain and the functionally modified CNTs strengthened hybrid composites were also characterized by measuring their fracture toughness. The fracture toughness was determined using notched specimen as shown in Fig. 26. The results are shown in

Fig. 27. The measured fracture toughness values showed 19% increase for the addition of 0.5 wt% CNTs over the plain GRP composites. The significant improvement in the impact properties and the energy absorption characteristics can be realized by adding a small quantity (0.1 wt%) of the functionalized MWCNTS. However, as the CNT weight fraction increased to 1 wt%, the fracture toughness values does not increase appreciably. The reasons behind this phenomenon can be attributed to CNT agglomerations as discussed before.

5. Conclusions and recommendations

Nano-strengthened hybrid GRP composites were mechanically characterized for different weight fraction of 0.1 wt%, 0.5 wt% and 1 wt% multiwall carbon nanotubes (MWCNTs) with 32 wt% of glass fiber mass fraction respectively. Before choosing the hybrid composites fabrication parameters, an optimum fiber mass fraction for the glass reinforced fiber composites (GRPs) were obtained by fabricating and mechanically testing the GRP composites with fiber mass fraction of 24 wt%, 32 wt% and 40 wt% respectively. From the tensile, flexural and impact properties results, the GRP composites with 32 wt% were found to be the most suitable mass fraction for fabricating the hybrid composites. Then a detailed study on the functionalization of MWCNTs with three functionalization time of 6 h, 24 h and 48 h, were carried out, to determine the optimum functionalization parameters without exfoliating the MWCNTs. Based on the results, the MWCNTs functionalized with nitric acid for 24 h were found to be the suitable functionalization time. From the above findings, the GRP hybrid composites with 32 wt% of glass fiber with three weight fraction of MWCNTs were fabricated.

The GRP hybrid composites were tested for their mechanical properties. The results shows that the GRP hybrid composites reinforced with 0.5 wt% functionalized CNTs are better than those of plain GRP, 0.1 wt% and 1 wt% of functionalized CNT composites. At high weight fraction of 1 wt% CNTs, agglomerations could not be prevented and this led to poor mechanical properties of the hybrid composites. In view of the above, it can be concluded that functionalization promotes homogeneous dispersion of CNTs within the matrix. In addition, it also promotes good interfacial adhesion between the matrix, reinforced fibers and the CNTs which is apparent from the experimental results. This technique may perhaps be extended to other polymer matrices. The similar hybridization technique can also further be extended to other fibers. One of the future recommendations is that the researches must focus on finding suitable fabrication methods for realizing the potential of CNTs as secondary reinforcements in hybrid composites.

Acknowledgment

The authors acknowledge the financial assistance support from National Research Foundation, South Africa

References

[1] Groover MP. Fundamental of modern manufacturing. John Wiley & Sons, Inc; 2000.
[2] Mangalgiri P. Composite materials for aerospace applications. Bull Mater Sci 1999;22(3):657–64.
[3] Kretsis G. A review of the tensile, compressive, flexural and shear properties of hybrid fibre-reinforced plastics. Composites 1987;18:13–23.
[4] Green P. Fibre volume fraction determination of carbon–epoxy composites using an acid digestion bomb. J Mater Sci Lett 1991;10:1162–4.
[5] Kretsis G. A review of the tensile, compressive, flexural and shear properties of hybrid fibre-reinforced plastics. Composites 1987;18:13–23.
[6] Karsli NG, Yesil S, Aytac A. Effect of hybrid carbon nanotube/short glass fiber reinforcement on the properties of polypropylene composite. Compos Part B: Eng 2014;63:154–60.
[7] Mansur HS, Pereira MM, Costa HS, Mansur AAP. Mechanical behavior of nanostructured hybrids based on poly(vinyl alcohol)/bioactive glass reinforced with functionalized carbon nanotubes. J Nanomater 2012;2012:1–9.
[8] Kickelbick G. Hybrid materials: synthesis, characterization and applications. Wiley-VCH Verlag GmbH & Co KGaA; 2007. p. 1–48.
[9] Mathur RB, Chatterjee S, Singh BP. Growth of carbon nanotubes on carbon fibre substrates to produce hybrid/phenolic composites with improved mechanical properties. Compos Sci Technol 2008;68:1608–15.
[10] Garcia EJ, Wardle BL, John Hart A, Yamamoto N. Fabrication and multifunctional properties of a hybrid laminate with aligned carbon nanotubes grown in situ. Compos Sci Technol 2008;68:2034–41.
[11] Iijima S. Helical microtubules of graphitic carbon. Nature 1991;354:56–8.
[12] Bachtold A, Hadley P, Nakanishi T, Dekker C. Logic circuits with carbon nanotube transistors. Science 2001;294:1317–20.
[13] McDonough JR, Choi JW, Yang Y, Mantia FL, Zhang Y, Cui Y. Carbon nanofiber super capacitors with large areal capacitances. Appl Phys Lett 2009;95:24309–11.
[14] Ajayan PM, Iijima S. Capillarity-induced filling of carbon nanotubes. Nature 1993;361:333–4.
[15] Xie XL, Mai YW, Ping X. Dispersion and alignment of carbon nanotubes in polymer matrix: a review. Mater Sci Eng 2005;R49:89–112.
[16] Saito R, Dresselhaus G, Dresselhaus MS. Physical properties of carbon nanotubes. UK: Imperial College Press; 1999.
[17] Alexander S, Stoddart FS, Steuerman D, Wong EW, Yang X, Chung SW, et al. Preparation and properties of polymer-wrapped single walled carbon nanotubes, 40. Wiley-VCH Verlag GmbH & Co KGaA; 2001 (9), p. 1721–5.
[18] Sun YP, Fu K, Lin Y, Huang W. Functionalized carbon nanotubes: properties and applications. Acc Chem Res 2002;35(12):1096–104.
[19] Lu KL, Lago RM, Chen YK, Green MLH, Harris PJF, Tsang SC. Mechanical damage of carbon nanotubes by ultrasound. Carbon 1996;34(6):816–74.
[20] Hirsch A. Functionalization of single-walled carbon nanotubes. Angew Chem Int Ed 2004;41:1853–9.
[21] Zhang X, Sreekumar TV, Liu T, Kumar S. Properties and structure of nitric acid oxidized single wall carbon nanotube films. J Phys Chem B 2004;108:16435–40.
[22] Yaping Z, Aibo Z, Qinghua C, Jiaoxia Z, Rongchang N. Functionalized effect of carbon nanotube/epoxy nano-composites. Mater Sci Eng 2006;435–436:145–9.
[23] Jacob MSD, Paskaramoorthy R. Double-wall carbon nanotube-reinforced polyester nanocomposites: improved dispersion and mechanical properties. Polym Compos 2012;33:866–71.
[24] Wang S. Optimum degree of functionalization for carbon nanotubes. Curr Appl Phys 2009;9:1146–50.